2023 IEEE International Conference on Robotics and Automation (ICRA 2023)
May 29 - June 2, 2023. London, UK

A fluidic actuator with an internal stiffening structure inspired by mammalian erectile tissue

Jan Fras and Kaspar Althoefer, *Senior Member, IEEE*

***Abstract*— One of the biggest problems with soft robots is precisely the fact that they are soft. Indeed the softer they are, the less force they can exert on the environment. Researchers have proposed a number of stiffening methods, but all of them have drawbacks, such as locking the shape of the device in a way that precludes further adjustments. In this paper we propose a stiffening method inspired by the internal structure of the mammalian penis. The soft actuation chamber is divided into small compartments that trap the actuation fluid, leading to locally amplified pressure increase under certain conditions. At the same time, the proposed solution does not affect the actuation mechanism, allowing the actuator to be adjusted in one direction just as if it was in non-stiffened mode, while offering a stiff response in the opposite direction. Our prototype achieves an increase in stiffening of approximately a factor of two. The paper describes the concept, the mathematical justification of the working principle, the prototype design, its implementation and our experimental results.**

I. Introduction

Soft robots have enormous potential in fields where interaction between device and environment needs to be gentle. They are compliant and adapt easily to surrounding objects - seemingly ideal alternatives to traditional rigid robots. The problem, however, is that for many potential applications, while there is a requirement for robot-environment interaction to be gentle and compliant, there is also a need for force exertion. A trade-off situation therefore exists between compliance and maintaining shape, position and force exertion. The goal is therefore to develop stiffening mechanisms that allow for an on-demand reduction in compliance in favour of an increase in strength.

One approach in soft robotics is to draw inspiration from nature, e.g., elephant trunks and octopus arms, both of which are soft-structured but able to stiffen and exert force when required. With this in mind, a range of bio-inspired stiffening mechanisms have been proposed.

These can be classified as 'passive stiffness change' or 'active stiffness change' systems. Passive stiffness change devices are those whose physical properties change as the device transits from one working state to another, i.e., soft to stiff and reverse. Active stiffness mechanisms often use an antagonistic approach whereby multiple actuation mechanisms work in collaboration to achieve movement and stiffening as required.

This work was supported by a research grant from the European Union in the framework of project STIFF-FLOP (FP7-ICT-287728).

[1]J. Fras and K. Althoefer are with the Centre of Advanced Robotics @ Queen Mary (ARQ), Faculty of Science and Engineering, Queen Mary University of London, London E1 4NS, UK j.fras@qmul.ac.uk, k.althoefer@qmul.ac.uk

One popular passive approach is known as jamming, in which structures are 'locked' by squeezing physical elements together so that the structure's body stiffens in response to the increased friction caused by the jamming force. There are various systems of this type, among them devices based on granular jamming [1], [2], [3], layer jamming [4], [5], [6] or jamming of macro-scale structural elements like scales or ossicles [7], [8].

Fig. 1: A subset of prototype actuators developed for this project.

Another approach is based on stiffness or state transition as a function of the temperature of the material used ([9], [10], [11], [12]). These methods, however, are energy-intensive and slow, due to lengthy heating and cooling cycles.

When using an antagonistic actuation method, considered an active stiffening approach, two or more actuators, arranged in an opposing way, act against each other and the stiffness change is achieved by increasing their actuation magnitude simultaneously to stiffen the associated joint.

Examples of such mechanisms are muscles powering joints in human bodies, or pneumatic actuators moving a rotary joint as presented in [13], [14]. Another approach uses pneumatic actuation to extend a chamber alongside a tendon pulling in the opposite direction, creating resultant stiffening when simultaneously actuated [15], [16]. On the downside, stiffening based on the antagonist principle requires redundancy as at least two actuation elements acting against one another are needed.

Recent research focuses on jamming as a route to improving the coupling of actuation and stiffening. As an example, in [5], particles are squeezed by expanding an actuation chamber. Similarly, in [17] an inflatable structure is equipped with patches composed of several layers connected via valves to the atmosphere and an internal chamber. These patches can be selectively jammed depending on the valve states. Better stiffness control can therefore be achieved as no energy source beyond the actuation mechanism itself is required.

The actuator we propose has an internal structure inspired by the corpus cavernosum sinusoids of the mammalian

penis [18], [19]. It is composed of individual compartments that trap the actuation fluid inside, increasing the bending resistance of the device. As the actuation chamber is divided into small distinct compartments, the local pressures in these compartments increase when the actuator is compressed due to an external force, resulting in an increase in stiffness. As with biological sinusoids during an erection, fluid flow in the proposed actuator is managed such that during actuation, fluid can flow in but not out, thereby trapping the fluid completely in the actuator. This new design allows for the coexistence of high compliance on actuation along with stiff response to a disturbance at any operating point. The stiffening mechanism does not lock the shape of the actuator. Despite the increased stiffness, the actuator can still adjust to external changes, such as the movement of the object it interacts with. When the object moves away, the actuator is able to follow its movement by allowing more actuation fluid to be pushed into the actuation chamber.

II. Materials and methods

A. Stiffening mechanism

Consider a flexible expanding actuation chamber with a mass of fluid trapped inside. In this scenario, in static conditions, there are three forces in equilibrium. They are the forces due to internal pressure, external disturbance, and internal stress resulting from the stretch of the material. As the trapped fluid has a constant mass, any external disturbance compressing it causes its volume to decrease, which in turn results in a pressure increase, affecting the stresses in the material and the equilibrium point. Effectively the apparent stiffness of such a structure is higher than it would be when the pressure, rather than its mass, was kept at a constant level.

Consider now an external force applied to a flexible but relatively non-stretchable cylinder filled with pressurised gas (see fig. 2a). If this external force is strong enough to overcome the internal pressure, the cylinder will deform. Due to the bending moment distribution along the cylinder's length, the deformation is more intense near the cylinder base, while less bending is observed close to the point at which the force is applied. As a result, the compression of the wall on the opposite side to the force application point is higher near the base (see fig. 2b). Consequently, the base's contribution to the internal volume compression is higher than that of the rest of the pressurised cylinder. If the external force exceeds a certain value, the cylinder begins to buckle, due to high strain concentration near the base, leading to a reduction in bending stiffness (see fig. 2c [20]).

There are several examples of soft bending actuators or soft manipulators in which the pressurised actuation medium can move freely within the actuation chamber so that the fluid compressed at any one point can move towards areas that are not exposed to an external force [21], [22], [23], [24], [25], [26]. In these cases, the impact of the force is most pronounced at the base of the device leading to more bending or even buckling near the base.

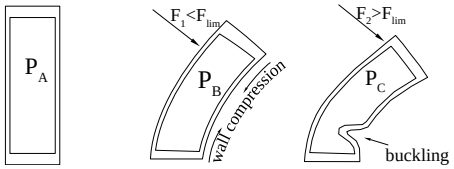

Fig. 2: An external disturbance on a pressurised cylinder. (a) passive state, (b) the bending motion causes the opposite cylinder side to shorten, the internal volume to shrink and the pressure to grow, (c) force value exceeds a specific value F_lim, no more wall compression is observed, but the structure starts t buckle instead. Internal pressure $P_A < P_B < P_C$.

When a pressurised medium is able to travel inside the actuation chamber, the actuator resistance remains low, as the local, relatively high volume compression (due to the external force) is spread evenly throughout the entire volume. This results in limited increase in overall pressure and stiffness. If, however, the gas compression was held within the area in which it originated, the resistance/stiffness of the actuator would be much more pronounced.

Therefore, by dividing an actuator chamber into smaller volumes - see fig. 3, such that the fluid is unable to move freely between compartments, the pressure increases proportionally to the local (rather than the global) volume change. The resulting pressure would not be homogeneous throughout the actuator, but would show a more pronounced increase closer to the base. Since the bending moment is greatest near the base, the actuator experiences the greatest volume compression in that area. As a consequence, the base of the actuator would stiffen more than the rest of its body, increasing the overall force response.

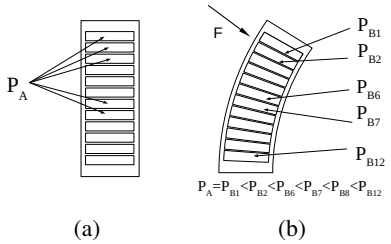

Fig. 3: In case the internal volume of the actuator is divided into small compartments, the compressed medium cannot move inside the actuator leading to pressure increase locally. Thanks to that, the resulting stiffness of the actuator is significantly higher, and buckling is prevented.

Our proposal is to divide the overall actuator into small compartments along its length and interconnect these compartments using directional valves that open when air streams in from the compartment closest to the actuator tip, and close if the air pressure in the compartment nearer the base increases, such as in response to an external force. In this way, the actuator can be easily filled with air from the top

but if an external force is applied, the valves close preventing air from flowing into more distal compartments. It is noted that air flow into more proximal compartments would also be impossible, as the pressure in the compartment nearer the base would be even higher. This blocking of air in local compartments leads to a local increase in pressure and an overall increase in stiffness of the actuator when experiencing an external force.

The final base compartment needs to be connected to the outside environment (i.e. the surrounding atmosphere) with a binary (on/off) valve to vent the overall structure. This valve would remain closed during operation and only opened to release the pressure and return the actuator to its 'relaxed' state.

B. Principle of stiffness increase

1) A linear actuator: Consider a flexible cylinder comprising an internal pneumatic chamber reinforced with helical fibre. Assuming the actuator's constituent elastic material shows a linear strain-stress behaviour, it will behave like a spring whose elongation is described by the spring equation - see fig. 4. The stiffness of such an actuator is determined by the spring constant k_0.

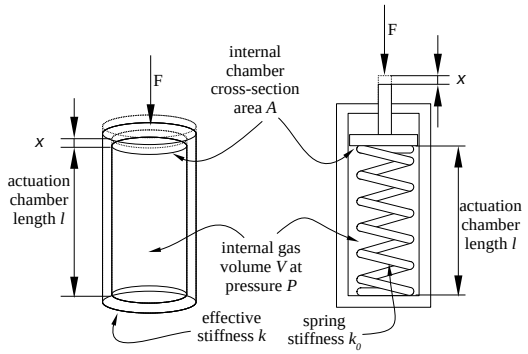

Fig. 4: The force response for external displacement. The cylindrical linear actuator and an equivalent pneumatic cylinder with a spring in parallel.

This cylinder, when pressurised under an external force could be described using eq. (1), where F_p and F_e represent pressure-induced force and external force values, respectively.

$$F_e - F_p = k_0 x \tag{1}$$

where F_p represents the pressure-related force and can be expressed as $F_p = AP$. A and P stand for the chamber cross-sectional area and relative internal pressure value.

The F_p value does not change under constant pressure inside the chamber. In that scenario, the device is powered via a pressure regulator that constantly adjusts to any value changes.

The situation changes if the pressure is initially set but not regulated thereafter. If the mass of the gas inside the chamber and the gas temperature remain constant, the pressures before and after any disturbance (P_0 and P_1 respectively) can be described by the ideal gas law $P_0V_0 = P_1V_1$. This in turn can be used to calculate pressure for a given displacement as shown here:

$$P(x) = \frac{V_0}{V_1}P_0 = \frac{l_{P_0}}{l_{P_0} - x}P_0 \tag{2}$$

Taking the above into account in relation to the closed chamber, eq. (1) can be reformulated as eq. (3) where A denotes the cross-sectional area of the actuator and P_e stands for the atmospheric pressure.

$$F_e + A(P_0\frac{l_{P_0}}{l_{P_0} - x} - P_e) = k_0 x \tag{3}$$

Effective stiffness k will therefore be represented by

$$k = \frac{\mathrm{d}F_e}{\mathrm{d}x} = k_0 + AP_0\frac{l_{P_0}}{(l_{P_0} - x)^2} \tag{4}$$

Given that the desired behaviour is the increase in stiffness, the stiffness gain can be expressed as:

$$\frac{k}{k_0} = 1 + \frac{AP_0 l_{P_0}}{k_0(l_{P_0} - x)^2} \tag{5}$$

where l_{P_0} is the length of the actuator pressurised with pressure $p = P_0$, before the external load is applied. Knowing the parameters of the material used, and the geometry of the actuator, that length can be expressed as a function of pressure as $l_P = l(P) = l_0 + \frac{PA}{k_0}$ where l_0 is the passive length of the device.

Assuming that the passive length and the fully extended length of actuator l_0 and l_{P_0} respectively, at a given pressure P_0 are predefined by the design requirements, we can express the required stiffness k_0 of the device as follows: $k_0 = A\frac{P_0 - P_e}{l_{P_0} - l_0}$.

Combining the above equation and eq. (5) we get:

$$\frac{k}{k_0} = 1 + \frac{(P_0 l_{P_0})(l_{P_0} - l_0)}{(P_0 - P_e)(l_{P_0} - x)^2} \tag{6}$$

which shows that the stiffness increase for an actuator with a predefined length and range is a function of the value of the pressure required to achieve that extension P_0. Stiffness increase for an actuator expanding twice ($l_{P_0} = 2l_0$) depending on the P_0 value and the compression value $\frac{x}{l_{P_0} - l_0}$ is presented in the plots of fig. 5.

The above reasoning demonstrates that the device's stiffness increases if the mass of the actuation gas is locked within the actuation chamber volume, but also that it is non-linear and increases with the compression of the device. The lower the actuation pressure required to achieve the assumed extension of the actuator, the more pronounced the increase in stiffness.

Taking all the above into account, the actuator design can be tuned to low actuation pressures (e.g. increasing the actuation chamber area) to increase its ability to stiffen when the actuation chamber is closed.

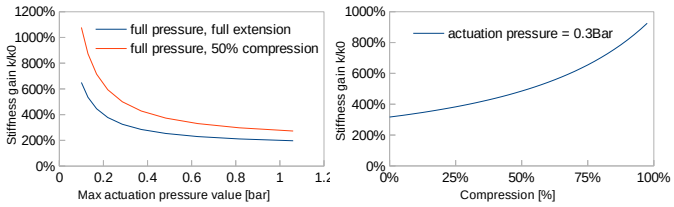

(a) (b)

Fig. 5: (a) Stiffness increase vs full actuation pressure for no compression and 50% compression of the device, (b) stiffness increase vs compression for 0.3 bar actuation pressure. Assumed nominal extension of the actuator is $l_{P_0} = 2l_0$ at pressure P_0.

2) A bending actuator: The bending actuator considered here uses similar physical principles, except that the elongation on one side of the actuator is constrained by a strain limiting layer. Similar reasoning can therefore be applied in relation to the bending motion.

In static conditions, the state of the actuator can be described via the equilibrium condition eq. (7), fig. 6.

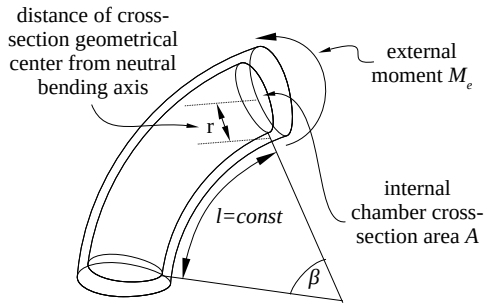

Fig. 6: Bending actuator geometry

$$M_p + M_e = M_s \tag{7}$$

where M_s denotes torque resulting from internal stresses $M_s = \beta EI$, and where β, E and I stand for bending angle, Young modulus and first moment of inertia of the cross-section of the device, respectively. M_p and M_e are the internal force moment and external moment resulting from the pressure inside and external force, respectively.

The apparent bending stiffness k_b of the device relates to the change of the external moment M_e, itself a function of change in bending angle causing a deviation, as follows:

$$k_b = \frac{\mathrm{d}M_e}{\mathrm{d}\beta} = \frac{\mathrm{d}(\beta EI - M_p)}{\mathrm{d}\beta} \tag{8}$$

The internal moment M_p depends on the chamber geometry and the internal pressure $M_p = ArP$. The pressure in turn is also affected by the volume change, and can be expressed in terms of the initial pressure and the current bending angle of the device, $P_1 = P_0 \frac{l+r\beta_{P_0}}{l+r+\beta_{P_1}}$. Consequently the derivative eq. (8) can be expressed as:

$$k_b = \frac{Ar^2 P_0 (l + r\beta_0)}{(l + r\beta_1)^2} + EI \tag{9}$$

Just as with the linear actuator, we can assume that l, EI and β_0 values are set by design requirements, while other values, A, r, and P_0 can be tuned to achieve the requisite bending and passive stiffness levels.

And similarly, we can plot the apparent stiffness gain with respect to the assumed pressure value P_0, fig. 7.

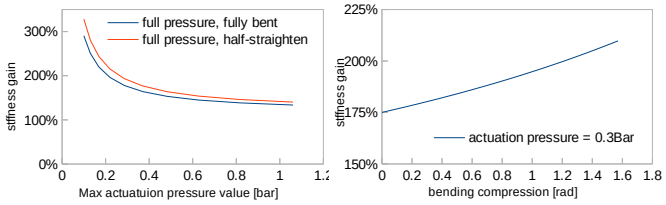

(a) (b)

Fig. 7: (a) Stiffness increase as a function of actuation pressure P_0 for fully bent and half straightened (with external force) device, (b) stiffness increase vs compression for 0.3 bar actuation pressure. Assumed nominal bending of the actuator is $\beta_{P_0} = \pi$ at pressure P_0.

The parameters used for generating the plots above are the actual values used for the prototype described in the following sections. Given the geometry of the actuator, the expected stiffness gain at actuation pressure of 0.3 bar is around 1.8 times the original stiffness and is expected to increase slightly on external disturbance.

C. Design

The core part of our design, and indeed the main difference with respect to previous soft actuator designs [22],[27], is the subdivision of the overall actuator structure into small actuation compartments using dividers. Each divider features a directional valve that allows the pressurised medium to flow in one direction only. The top compartment is supplied with the actuation pressure, while the bottom one (binary on/off valve) can be opened or closed to vent the device or to keep it pressurised.

Each valve requires some small pressure difference to open, and the overall pressure drop we observed between the first and the last compartment in first prototypes was considerable. For that reason, to ensure that the actuation pressure is achieved evenly throughout all actuator compartments, directional valves between the compartments, in addition to those connecting each of the compartments with the pressure supply, were embedded - see fig. 8. Given that each compartment is pressurised equally, we can assume that the actual actuation pressure is virtually the same as the supply pressure.

Pressurisation and venting cycles, as well as the valves' working principle, are depicted in fig. 9. The valves are created by overlaying a small hole with a thin silicone membrane. Since the silicone membrane tends to adhere to

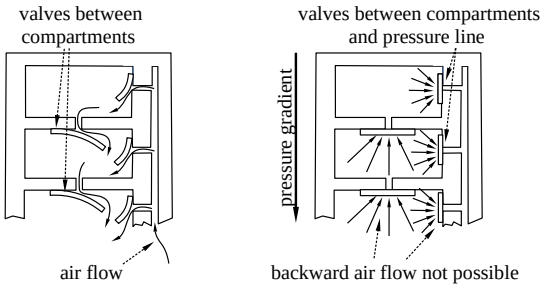

(a) (b)

Fig. 8: The two sets of directional valves, those between compartments and those connecting to the supply pressure channel ensure adequate distribution of the actuation pressure throughout all compartments, whilst blocking air trying to move from proximal to distal compartments; (a) the differential valves enable the flow from the supply channel and from top to base; (b) but restrict flow in the opposite direction.

the material surrounding the hole, it creates a seal when there is pressure from outside. However, when there is pressure from within, acting on the membrane through the hole, the slight adhesion is overcome, and the membrane deflects, opening up the channel. Once the flow stops, the membrane re-seals the hole.

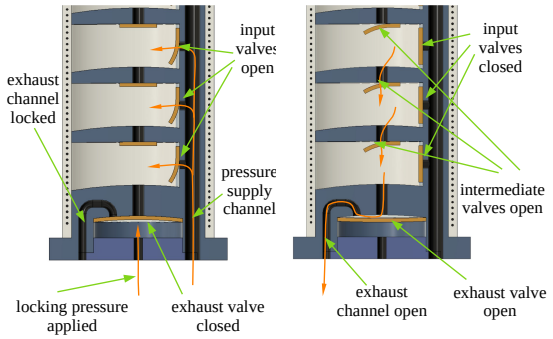

(a) (b)

Fig. 9: Actuation cycle: (a) pressurization, (b) venting.

D. Fabrication

A prototype was designed for casting silicone in 3D-printed moulds. The fabrication process consists of the following steps - creation of the external sleeve containing the reinforcing fibres, moulding of the internal structure, arrangement of the membranes constituting the internal valves, and assembly of all the parts.

The external sleeve is made in three steps. Initially, the thread is wrapped around a cylinder, then placed into a mould and covered with a layer of silicone. Once the silicone has cured, the cylinder is replaced with another cylinder of smaller diameter and an internal layer of silicone is created. When the internal silicone is cured, the resulting structure is cut along a straight line and peeled off the cylinder. For the external sleeve, SmoothOn Ecoflex 0030 silicone was used.

The internal structure is moulded in a multi-part mould using relatively stiff silicone SmoothOn Smooth Sill 950. Once out of the mould, uncured silicone is dispensed with a brush onto the surface areas surrounding the holes in order to create a smooth surface - a necessary step to ensure valves are airtight once fitted. Once surfaces have been prepared, small pieces of soft silicone sheeting are placed on top of each of the holes to create the actual valves; the internal structure of a physical prototype is shown in fig. 10(a). Initially, silicone glue was used to attach the sheeting on one side, but it turned out that the adhesion forces of the smooth silicone surfaces are high enough to keep them attached to the divider's structure

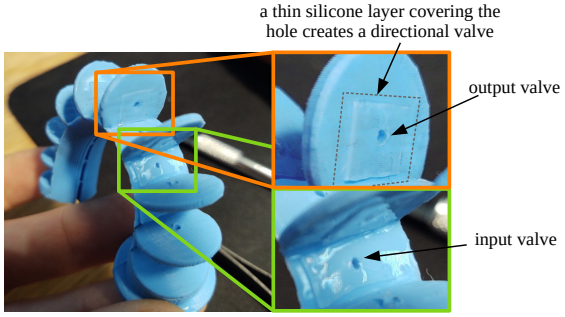

Fig. 10: (a) Implementation of the valves. Input and output valves exposed.

The final step is to apply the prepared external layer. For that process, glue is applied to the edge of all the dividers to ensure each compartment is appropriately sealed and that the medium can only flow through the directional valves. The finished actuator is shown in fig. 11.

(a) (b)

Fig. 11: Finished actuator, (a) passive state, (b) actuated.

III. Results

Experimental data was collected as described below.

A. Force response

The test setup consisted of two pressure regulators controlling the pressure inside the actuation chamber and the outlet valve, a Cartesian positioning system with a force sensor attached that is used to create the deflection and measure the reaction forces, and all the electronics required to actuate and record the data including an Arduino and Raspberry Pi boards. As a positioning system, an adapted Saintsmart CNC3018 machine was used. For experimental reasons, the

original spindle was replaced with a Robotous RFT40-SA01 force/torque sensor to collect the force data.

The test procedure involved actuation up to the requisite pressure value of 0.3 bar, closing the main venting valve with 1.2 bar pressure so that the pressurised medium could not escape, moving the force sensor along the predefined trajectory and recording the reaction forces of the actuator with respect to the position of the force sensor. This procedure was repeated in several trials to cover the whole sampling area. The pressure in each trial was set to the same value.

For the test setup and representation of the sampling points, as well as the trajectory of the probe see fig. 12. The normal force value as a function of XY (probe position) in relation to the actuator base is shown in fig. 13.

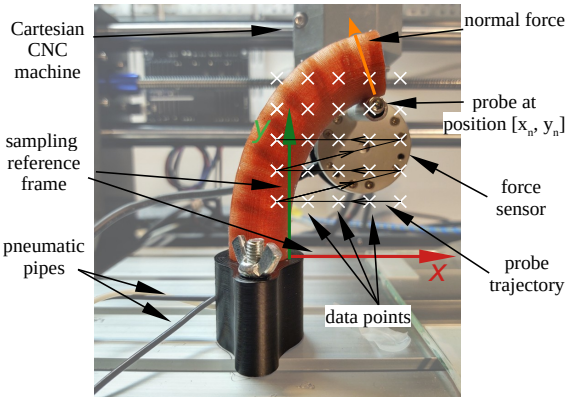

Fig. 12: The test setup used for data collection.

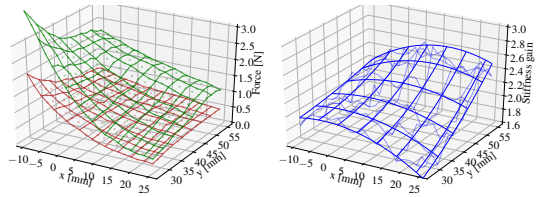

(a) (b)

Fig. 13: Normal force value with respect to the probe position for a fully actuated finger. (a) The samples have been collected for the stiffening mechanism engaged (green) and disengaged (red). (b) The relation between engaged and disengaged stiffening system force response - stiffness gain.

B. Grasping force

The force response presented in the previous section accounts for the force applied in the normal direction with respect to the deformed finger axis. In a real-world scenario, there would be more than one finger acting in opposition, cancelling the opposing vector components, but in such cases, the friction of the finger would also be significant. In our test, the probe was attached via ball bearings to ensure relatively friction-less operation to minimise that effect. However, if we assume some friction coefficient, the actual force required to pull out an object from a gripper composed of such fingers can be calculated - see fig. 14.

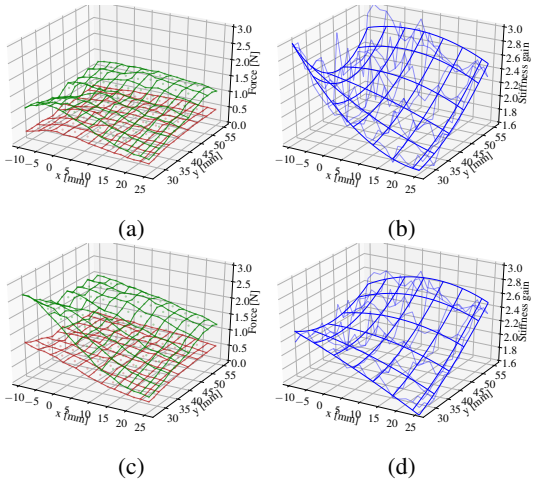

(a) (b) (c) (d)

Fig. 14: Force required to displace an object out of the gripper as a function of the location of the object with respect to the finger. (a) & (c) the calculated forces, (green with stiffening system engaged and red - disengaged), (b) & (d) grasping force gain. The data was plotted assuming friction coefficients: 0.1 and 0.5 for (a) & (b) and (c) & (d) respectively.

C. Discussion

In fig. 13, a lower value of x corresponds to greater displacement of the actuator with the probe, while a lower value of y indicates closer proximity of the probe to the base. The measured stiffness change falls within the expected range of 1.8 to 2.6, as shown in fig. 5. The gathered data reveals that the stiffness gain increases with the distance from the base, indicating that the internal structure provides greater benefit when the disturbance is applied further away or when the actuator is longer. Moreover, the gain increases with the disturbance (small x values) for short distances from the base (small y values), but decreases with the disturbance on the further end of the actuator (large y values).

D. Conclusion

In this work, we proposed an internal structure for fluidic soft actuators that can significantly improve the apparent stiffness of these devices while keeping their actual stiffness and actuation pressure within desired levels. We designed, manufactured and tested a proof-of-concept prototype. The experiments conducted produced results similar to what we expected based on calculations, showing a significant improvement in force response when the stiffening mechanism was engaged. The proposed actuator can be utilised in several designs but is especially suitable for soft gripper fingers. Its principal distinguishing characteristic is that actuation and stiffening work in a complementary way, without influencing each other. Because of this, actuation can proceed even when stiffening is engaged, as more actuation fluid is freely transferred into the actuation chamber. In other designs stiffening inhibits further actuation.

REFERENCES

[1] Vincent Wall, Raphael Deimel, and Oliver Brock. Selective stiffening of soft actuators based on jamming. In *2015 IEEE International Conference on Robotics and Automation (ICRA)*, pages 252–257. IEEE, 2015.

[2] Yonghua Chen, Yunquan Li, Yingtian Li, and Yizhong Wang. Stiffening of soft robotic actuators—jamming approaches. In *2017 IEEE International Conference on Real-time Computing and Robotics (RCAR)*, pages 17–21. IEEE, 2017.

[3] Huy Hoang Huynh, Dong Han, Kazuhiro Yoshida, Michael De Volder, and Joon-wan Kim. Soft actuator with switchable stiffness using a micropump-activated jamming system. *Sensors and Actuators A: Physical*, page 113449, 2022.

[4] Inrak Choi, Nick Corson, Lizzie Peiros, Elliot W Hawkes, Sean Keller, and Sean Follmer. A soft, controllable, high force density linear brake utilizing layer jamming. *IEEE Robotics and Automation Letters*, 3(1):450–457, 2017.

[5] Yingtian Li, Yonghua Chen, Yang Yang, and Ying Wei. Passive particle jamming and its stiffening of soft robotic grippers. *IEEE Transactions on robotics*, 33(2):446–455, 2017.

[6] A Clark and N Rojas. Design and workspace characterisation of malleable robots.

[7] SM Hadi Sadati, Yohan Noh, S Elnaz Naghibi, Althoefer Kaspar, and Thrishantha Nanayakkara. Stiffness control of soft robotic manipulator for minimally invasive surgery (mis) using scale jamming. In *International Conference on Intelligent Robotics and Applications*, pages 141–151. Springer, 2015.

[8] Hwayeong Jeong and Jung Kim. Echinoderm inspired variable stiffness soft actuator with connected ossicle structure. In *2019 International Conference on Robotics and Automation (ICRA)*, pages 7389–7394. IEEE, 2019.

[9] Francesco Visentin, Saravana Prashanth Murali Babu, Fabian Meder, and Barbara Mazzolai. Selective stiffening in soft actuators by triggered phase transition of hydrogel-filled elastomers. *Advanced Functional Materials*, 31(32):2101121, 2021.

[10] Yegor Piskarev, Jun Shintake, Vivek Ramachandran, Neil Baugh, Michael D Dickey, and Dario Floreano. Lighter and stronger: Cofabricated electrodes and variable stiffness elements in dielectric actuators. *Advanced Intelligent Systems*, 2(10):2000069, 2020.

[11] Yegor Piskarev, Jun Shintake, Christophe Chautems, Jonas Lussi, Quentin Boehler, Bradley J Nelson, and Dario Floreano. A variable stiffness magnetic catheter made of a conductive phase-change polymer for minimally invasive surgery. *Advanced Functional Materials*, page 2107662, 2022.

[12] Tingchen Liao, Manivannan Sivaperuman Kalairaj, Catherine Jiayi Cai, Zion Tsz Ho Tse, and Hongliang Ren. Fully-printable soft actuator with variable stiffness by phase transition and hydraulic regulations. In *Actuators*, volume 10, page 269. Multidisciplinary Digital Publishing Institute, 2021.

[13] Victoria Oguntosin, Ayoola Akindele, and Enock Oladimeji. Gesture-based control of rotary pneumatic soft robot using leap motion controller. In *2019 6th International Conference on Soft Computing & Machine Intelligence (ISCMI)*, pages 169–174. IEEE, 2019.

[14] Nathan S Usevitch, Allison M Okamura, and Elliot W Hawkes. Apam: antagonistic pneumatic artificial muscle. In *2018 IEEE International Conference on Robotics and Automation (ICRA)*, pages 1539–1546. IEEE, 2018.

[15] A. Stilli, H. A Wurdemann, and K. Althoefer. Shrinkable, stiffness-controllable soft manipulator based on a bio-inspired antagonistic actuation principle. In *International Conference on Intelligent Robots and Systems*, pages 2476–2481. IEEE, 2014.

[16] Ali Shiva, Agostino Stilli, Yohan Noh, Angela Faragasso, Iris De Falco, Giada Gerboni, Matteo Cianchetti, Arianna Menciassi, Kaspar Althoefer, and Helge A Wurdemann. Tendon-based stiffening for a pneumatically actuated soft manipulator. *IEEE Robotics and Automation Letters*, 1(2):632–637, 2016.

[17] Brian H Do, Valory Banashek, and Allison M Okamura. Dynamically reconfigurable discrete distributed stiffness for inflated beam robots. *arXiv preprint arXiv:2002.04728*, 2020.

[18] DA Kelly. Axial orthogonal fiber reinforcement in the penis of the nine-banded armadillo (dasypus novemcinctus). *Journal of Morphology*, 233(3):249–255, 1997.

[19] Kirk A. Keegan and David F. Penson. Chapter 28 - vasculogenic erectile dysfunction. In Mark A. Creager, Joshua A. Beckman, and Joseph Loscalzo, editors, *Vascular Medicine: A Companion to Braunwald's Heart Disease (Second Edition)*, pages 341 – 348. W.B. Saunders, Philadelphia, second edition edition, 2013.

[20] S.L. Veldman, O.K. Bergsma, and A. Beukers. Bending of anisotropic inflated cylindrical beams. *Thin-Walled Structures*, 43(3):461–475, 2005.

[21] A. Stilli, L. Grattarola, H. Feldmann, H. A. Wurdemann, and K. Althoefer. Variable stiffness link (vsl): Toward inherently safe robotic manipulators. In *2017 IEEE International Conference on Robotics and Automation (ICRA)*, pages 4971–4976, May 2017.

[22] J. Fras, J. Czarnowski, M. Macias, J. Glowka, M. Cianchetti, and A. Menciassi. New stiff-flop module construction idea for improved actuation and sensing. In *International Conference on Robotics and Automation*, pages 2901–2906. IEEE, 2015.

[23] J. Fras, M. Macias, Y. Noh, and K. Althoefer. Fluidical bending actuator designed for soft octopus robot tentacle. In *2018 IEEE International Conference on Soft Robotics (RoboSoft)*, pages 253–257. IEEE, 2018.

[24] P. Polygerinos, Z. Wang, J. T. B. Overvelde, K. C. Galloway, R. J. Wood, K. Bertoldi, and C. J. Walsh. Modeling of soft fiber-reinforced bending actuators. *IEEE Transactions on Robotics*, 31(3):778–789, June 2015.

[25] B. Mosadegh, P. Polygerinos, C. Keplinger, S. Wennstedt, et al. Pneumatic networks for soft robotics that actuate rapidly. *Advanced Functional Materials*, 24(15):2163–2170, 2014.

[26] Koichi Suzumori, Satoshi Endo, Takefumi Kanda, Naomi Kato, and Hiroyoshi Suzuki. A bending pneumatic rubber actuator realizing soft-bodied manta swimming robot. In *Robotics and Automation, 2007 IEEE International Conference on*, pages 4975–4980. IEEE, 2007.

[27] J. Fras and Kaspar Althoefer. Soft fiber-reinforced pneumatic actuator design and fabrication: Towards robust, soft robotic systems. In *Annual Conference Towards Autonomous Robotic Systems*, pages 103–114. Springer, 2019.